Bearing fault diagnosis based on spectrum images of vibration signals

OPEN ACCESS
IOP Publishing
Measurement Science and Technology
Meas. Sci. Technol. **27** (2016) 035005 (10pp)
doi:10.1088/0957-0233/27/3/035005

Bearing fault diagnosis based on spectrum images of vibration signals

Wei Li, Mingquan Qiu, Zhencai Zhu, Bo Wu and Gongbo Zhou

School of Mechatronic Engineering, China University of Mining and Technology, Xuzhou 221116, People's Republic of China

E-mail: liwei_cmee@163.com

Received 8 November 2015, revised 20 December 2015
Accepted for publication 4 January 2016
Published 2 February 2016

Abstract

Bearing fault diagnosis has been a challenge in the monitoring activities of rotating machinery, and it's receiving more and more attention. The conventional fault diagnosis methods usually extract features from the waveforms or spectrums of vibration signals in order to correctly classify faults. In this paper, a novel feature in the form of images is presented, namely analysis of the spectrum images of vibration signals. The spectrum images are simply obtained by doing fast Fourier transformation. Such images are processed with two-dimensional principal component analysis (2DPCA) to reduce the dimensions, and then a minimum distance method is applied to classify the faults of bearings. The effectiveness of the proposed method is verified with experimental data.

Keywords: vibration signal, fault diagnosis, bearing, image

(Some figures may appear in colour only in the online journal)

1. Introduction

Bearings are the most commonly used components in rotating machinery, and bearing faults may result in significant breakdowns, and even casualties [1–3]. Statistics show that bearing failure is about 40% of the total failures of induction motors [4], and is the leading contributor of gearbox faults in wind turbines [5]. Hence, it is important to diagnose bearings.

Fault diagnosis of bearings is usually based on vibration signals, and a set of features are extracted in order to classify the faults [6]. The features could be in the time domain, frequency domain or time-frequency domain [7], such as peak amplitude, root-mean-square amplitude, skewness, kurtosis, correlation dimension, fractal dimension, Fourier spectrum, cepstrum, or envelope spectrum [8, 9]. These features are generally in forms of scalar or vector. There are some specific descriptions of waveform in the time domain and some parameters of spectrum in the frequency domain. A single feature only describes one aspect of vibration signals. Therefore, many works combine more than one feature to improve the performance of fault diagnosis. For example, Khelf *et al* [10] performed fault diagnosis for rotating machines with several selected, relevant features by doing indicators ranking according to a filter evaluation. And many other artificial intelligence methods for fault diagnosis have made full use of multi-features in time domain, frequency domain and time-frequency domain, so as to improve the diagnostic performance [11–16].

The main way humans recognize different objects is using vision, and the simplest form of vision is an image. Rich information can be included in an image. Time domain and frequency domain features represent some characteristics of vibration signals. An image can give a comprehensive description of vibration signals, including much more information about the bearings. Computer vision techniques have been well developed and applied for image processing and recognition [17–20]. Recently computer vision techniques were also further applied in the field of fault diagnosis [21, 22]. In [21], an object detection method was used to detect specific lines in the time-frequency image of bearing vibration signals. In [22], an image processing method was employed to enhance the fault features in spectrograms of aircraft engines.

In this paper, we propose a novel fault diagnosis method using the spectrum image of vibration signal as the feature. The spectrum images of normal bearings and faulty bearings

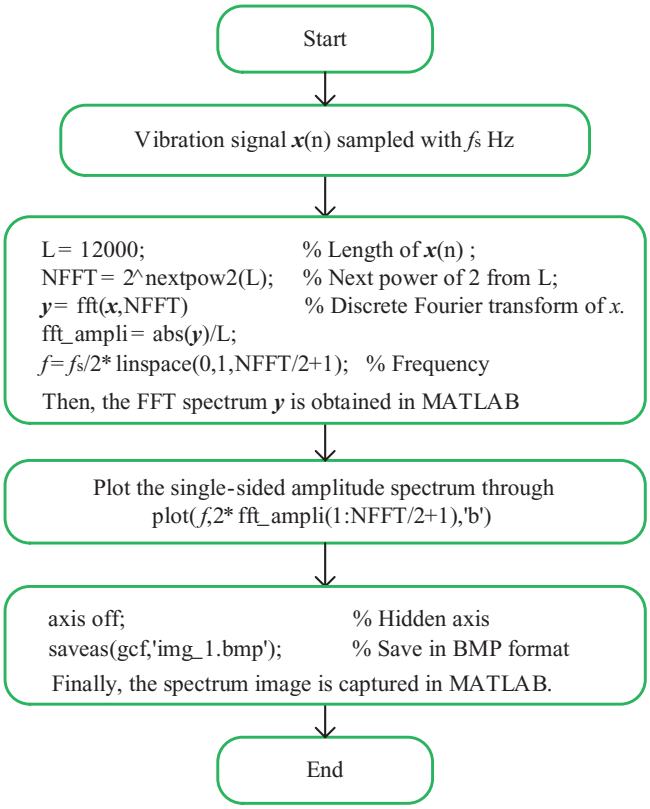

Figure 1. Flow chart of image creation in MATLAB.

are obtained based on the fast Fourier transformation (FFT) of vibration signals, where all images are of the same sizes, in pixels. We use two-dimensional principal component analysis (2DPCA) to process the images in order to reduce their dimensions and obtain the so-called eigen images, and then we classify the bearing faults with the help of a minimum distance method.

The rest of this paper is organised as follows. Section 2 presents the fault diagnosis method based on spectrum images, including image creation, image processing and image recognition. Section 3 gives the experimental results. Finally, the conclusion is given in section 4.

2. Fault diagnosis based on spectrum images

2.1. Image creation with FFT

There are many possible choices for the creation of vibration signal images. The images can be obtained in time domain, frequency domain, and time-frequency domain. In this study, we capture the FFT spectrums of vibration signals as images. The x-axis of the spectrum is frequency in Hertz, and the y-axis is the amplitude. For a given signal, the x-axis of the spectrum is determined by the sampling rate. When capturing the spectrum, its y-axis is auto-scaled. Then the parameter of the image is just the size (in pixels). With a larger image, more details of the spectrum can be depicted; while with a smaller image, some details may be lost. The flowchart of image creation in MATLAB is detailed illustrated in figure 1.

By taking such images as the features of vibration signals, we actually make use of all information contained in the spectrum – i.e., characteristic frequencies and harmonics of bearings, the geometrical structure of the spectrum, the peak amplitude of the spectrum and so on. The images provide much more useful knowledge of bearings, and we can also take advantage of the well developed computer vision technique to realize fault diagnosis. Next, two-dimensional principal component analysis (2DPCA) is applied to process the obtained spectrum images such that the low dimensional features of the images can be obtained.

2.2. Image processing

2DPCA is a feature projection method similar in principle to the conventional principal component analysis (PCA), using which we can extract the intrinsic information of images with a direct operation on the matrix. The 2DPCA projection process can be summarized as follows [23].

- *Step* 1 : Suppose that there are M training image samples, and the jth training image(with $w \times h$ pixels) is denoted by an $w \times h$ matrix $A_j, j = 1, 2, \ldots, M$. The average image of all the training image samples is denoted by $\overline{A}$. Then the global image scatter matrix G can be evaluated by

$$G = \frac{1}{M}\sum_{j=1}^{N}(A_j - \overline{A})^T(A_j - \overline{A}) \in \mathbf{R}^{h\times h} \tag{1}$$

  where $(\bullet)^T$ represents the transpose of matrix $(\bullet)$.
- *Step* 2 : In order to obtain the basis vectors, it is necessary to find the eigenvectors u_k and eigenvalues λ_k of the global image scatter matrix G by solving the following equation:

$$Gu = \lambda u \tag{2}$$

  where $\lambda_k, k = 1, 2, \ldots, h$, are the eigenvalues, and $u = [u_1, u_2, \ldots, u_h]$ are the corresponding eigenvectors of G. To reduce dimensions, and decrease computational expense, we next normalise and sort the eigenvectors u in decreasing order according to the corresponding eigenvalues λ_k. Then the $u = [u_{\max 1}, u_{\max 2}, \ldots, u_{\max h}]$ and the corresponding eigenvalues $\lambda = [\lambda_{\max 1}, \lambda_{\max 2}, \ldots, \lambda_{\max h}]$ can be obtained. Here λ_k satisfies the following constraint:

$$\lambda_{\max 1} > \lambda_{\max 2} > \ldots > \lambda_{\max h}$$

- *Step* 3 : In order to obtain the optimal projection vectors, the first $d(d < h)$ largest eigenvectors are selected to form the projection basis as

$$U = [u_{\max 1} \quad u_{\max 2} \quad \cdots \quad u_{\max d}] \tag{3}$$

- *Step* 4 : Feature extraction is implemented with the projection basis obtained in the previous step. For a given image sample B, which is also the same size of $w \times h$ pixels corresponding to A_j, let

$$Y_k = BU_k \tag{4}$$

  where, $U_k = u_{\max k}$, and $k = 1, 2, \ldots, d$. Then the projected feature vectors, $Y_1, Y_2, \ldots, Y_d$ can be obtained - these are called the principal components of the image sample B. At last we can obtain the eigen image of B in the form of

$$E = [Y_1, Y_2, \ldots, Y_d] \in \mathbf{R}^{w \times d} \tag{5}$$

2.3. Image recognition

In order to classify the bearing faults, spectrum images of different faulty bearings must be recognized. Firstly some training image samples are processed through 2DPCA to obtain the corresponding eigen images of vibration signals with different faults. Then a nearest neighbor classification method is utilized for the classification of testing spectrum images.

Suppose that the ith projection feature matrix of the M training image samples is $E_i = [Y_1^{(i)}, Y_2^{(i)}, \ldots, Y_d^{(i)}]$, where $i = 1, 2, \ldots, M$, and that of the jth testing image is $T_j = E_j = [Y_1^{(j)}, Y_2^{(j)}, \ldots, Y_d^{(j)}]$. Here we apply Euclidean distance [24] to measure the distance between E_i and T_j as follows

$$d_i(E_i, T_j) = L_{p=2}(E_i, T_j) = \sum_{r=1}^{d} \| Y_r^{(i)} - Y_r^{(j)} \|_2 \tag{6}$$

where $\| Y_r^{(i)} - Y_r^{(j)} \|_2$ denotes the Euclidean distance between $Y_r^{(i)}$ and $Y_r^{(j)}$, and $Y_r^{(i)}$, $Y_r^{(j)}$ are the rth vector of E_i and T_j.

Suppose $L = s_1, s_2, \ldots, s_N, (N \leqslant M)$ is the category label set of the M training samples. In order to classify the jth testing image, it is necessary to find the subscript η, which satisfies

$$d_\eta = \min(d_i) \tag{7}$$

Then if the ηth training image is assigned as $s_k (s_k \in L)$, the jth testing image is classified as s_k.

2.4. Main procedure of the method

The main procedure of fault diagnosis process based on spectrum images is summarized as follows.

- *Data Acquisition:* The spectrum images of vibration signals are firstly created through FFT as described in section 2.1. The image database can be constructed with these spectrum images.
- *Eigen-images Extraction:* Once the image database is set up, the eigen images can be obtained through 2DPCA, as detailed in section 2.2.
- *Fault Classification:* A testing spectrum image can be classified by comparing with training spectrum images using the method given in section 2.3.

The flow chart of bearing fault diagnosis based on spectrum images is shown in figure 2.

3. Experimental results

In order to verify the effectiveness of the proposed fault diagnosis method, vibration signals from the bearing data centre of Case Western Reserve University are used [25]. The test stand consists of a driving motor, a 2 hp motor for loading, a torque transducer/encoder, accelerometers and control electronics. The test bearings support the motor shaft. With the help of electrostatic discharge machining, inner-race faults (IF), outer-race faults (OF) and ball faults (BF) of different sizes (0.007in, 0.014in, 0.021in and 0.028in) are made. The vibration signals are collected using accelerometers attached to the housing with magnetic bases, and four load conditions with different rotating speeds were considered, i.e. Load0 = 0 hp/1797 rpm, Load1 = 1 hp/1772 rpm, Load2 = 2 hp/1750 rpm and Load3 = 3 hp/1730 rpm. The vibration signals of normal bearings (NO) under different load conditions were also collected.

Rotating machinery usually works under different loads and speeds. In practice it is common to obtain features of faults under a certain load condition. Hence the vibration signals with two fault sizes (0.014in and 0.021in) under all four load conditions are used to demonstrate the effectiveness of the proposed method, where the training images of IF, OF and BF are created from one load condition (called training load condition) and the testing images are from all four load conditions (called testing load condition). In total, eight different tests are carried out, as shown in table 1, to classify the faults of bearings.

The FFT spectrum of each vibration signal is computed, using 1024 sampling points. The y-axis of the spectrum is auto-scaled. Then the spectrum is captured as an image of 420×560 pixels. Figures 3–6 show the spectrum images of a normal bearing and faulty bearings with fault size being 0.014in. Four hundred spectrum images are generated for normal bearing (NO) and faulty bearings (IF, BF or OF) under each load condition. The training images of normal bearings and faulty bearings are selected randomly under the training load condition, and all 400 spectrum images under each testing load condition are used for verification. Each test in table 1 is performed 20 times and the average classification rate is obtained.

In order to demonstrate the effectiveness of the proposed method, the spectrum images are processed through PCA and 2DPCA, and the classification results between them are compared.

3.1. Results based on PCA

The tests are firstly demonstrated with PCA. According to the feature dimensionality reduction criterion in [26], the so-called contribution of selected components with 20%, 40%, 60%, 80%, 90% and 100% are firstly performed to determine the reduced dimension. Thereafter, dimension reduction with 90% is designated in our research, as this was the case in which the average classification rate was the highest. The experimental results are shown in tables 2 and 3.

From table 2 we can see that the classification rates are mostly larger than 90%, but the classification rates of several tests are relatively low. For example, we only obtain a classification rate of about 75% when using images under Load1 as training data and images under Load3 as testing data. The actual output with $n = 3$ in this case is shown as figure 7. We can see intuitively that the IF (target output is: 2) images are classified incorrectly. Some testing images of IF are categorized into BF (target output is: 3), and the others are categorized into OF (target output is: 4), incorrectly. Through

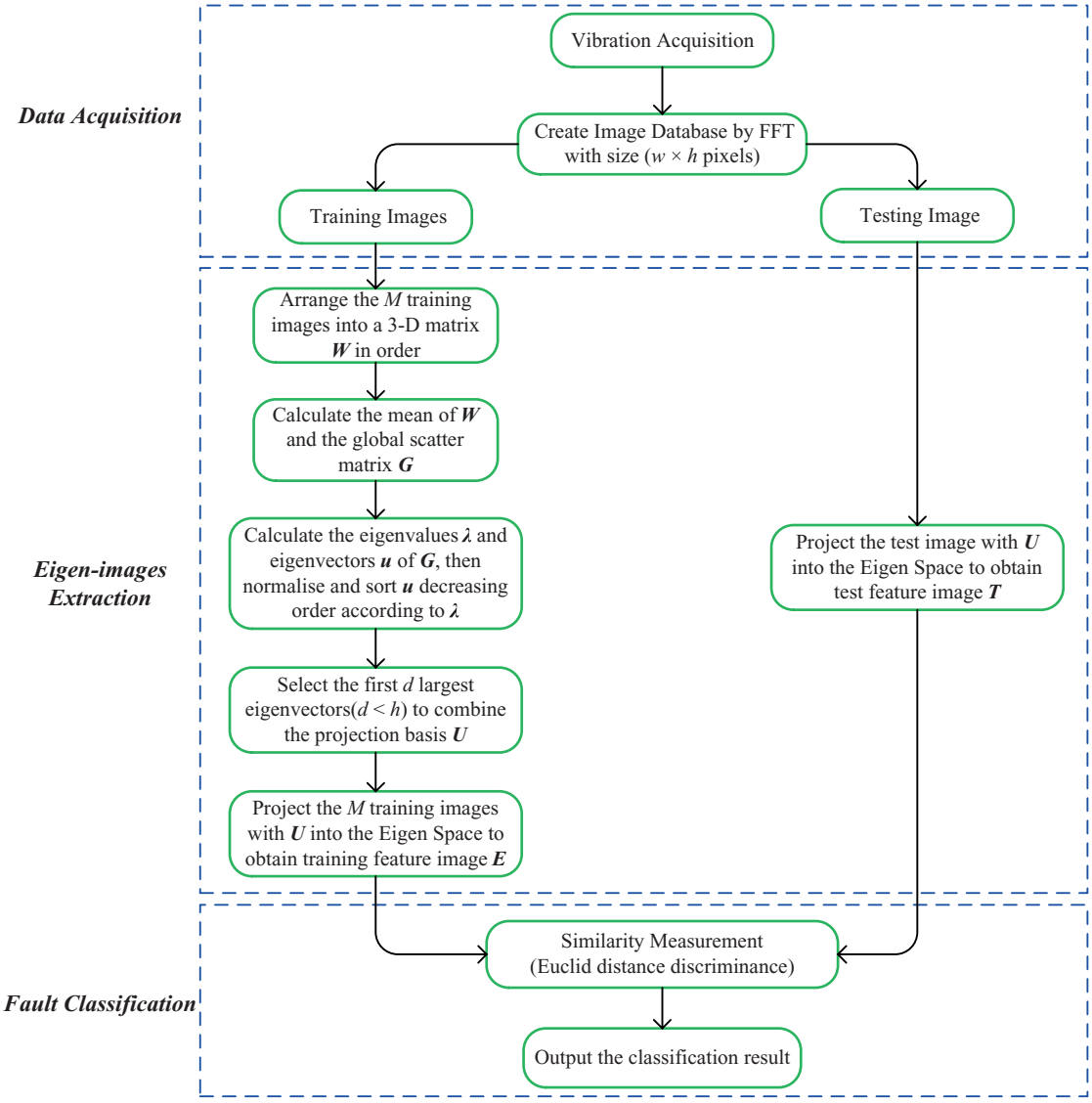

Figure 2. Flow chart of bearing fault diagnosis based on spectrum images.

Table 1. Description of the experiment setup.

# of test	Training	Testing	Fault type	Fault size
1	Load0	Load0, Load1, Load2, Load3	IF, BF, OF, NO	0.014in
2	Load1	Load0, Load1, Load2, Load3	IF, BF, OF, NO	0.014in
3	Load2	Load0, Load1, Load2, Load3	IF, BF, OF, NO	0.014in
4	Load3	Load0, Load1, Load2, Load3	IF, BF, OF, NO	0.014in
5	Load0	Load0, Load1, Load2, Load3	IF, BF, OF, NO	0.021in
6	Load1	Load0, Load1, Load2, Load3	IF, BF, OF, NO	0.021in
7	Load2	Load0, Load1, Load2, Load3	IF, BF, OF, NO	0.021in
8	Load3	Load0, Load1, Load2, Load3	IF, BF, OF, NO	0.021in

observing and analyzing the spectrum images of IF (Load3) and BF (Load1) carefully, it is plausible that the spectrum images of IF (Load3), BF (Load3) and BF (Load1) looked very similar, which resulted in the low classification rate.

Similar tests are carried out on the spectrum images with fault size being 0.021, and the classification results are presented in table 3. We can observe that the overall classification rate is higher than the classification rate with fault size 0.014. It is worth mentioning that an acceptable classification rate can be achieved by using only a single training image ($n = 1$).

3.2. Results based on 2DPCA

Having tested the performance of the 2DPCA based method with different dimension reduction, we determined $d = 10$ defined in formula (3) as the best selection. The diagnostic results with 2DPCA for fault size being 0.014 and 0.021 are given in tables 4 and 5. Taking Load0 as training samples, the classification rate could reach 100% with $n = 5$. When the

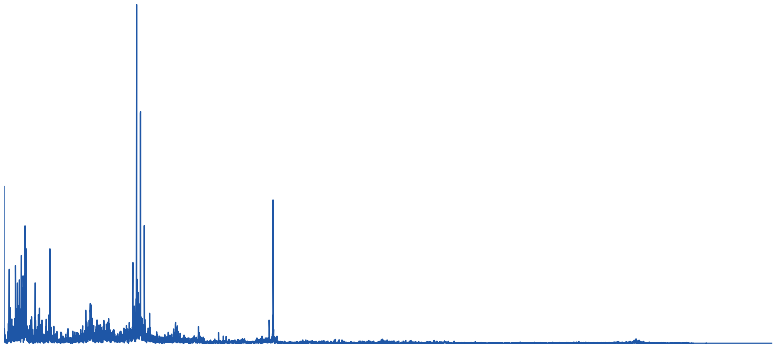

Figure 3. The FFT spectrum image of a normal signal.

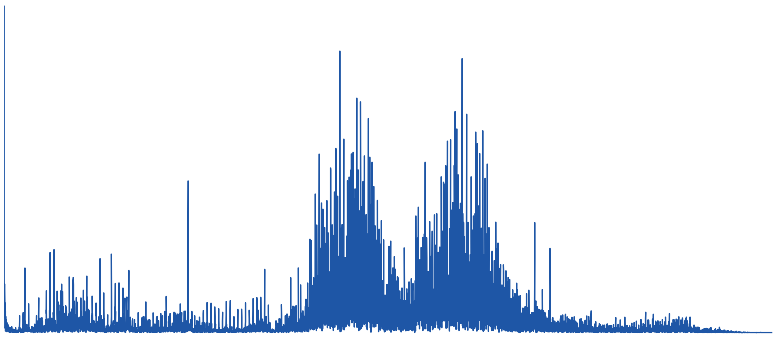

Figure 4. The FFT spectrum image of an inner-race fault signal.

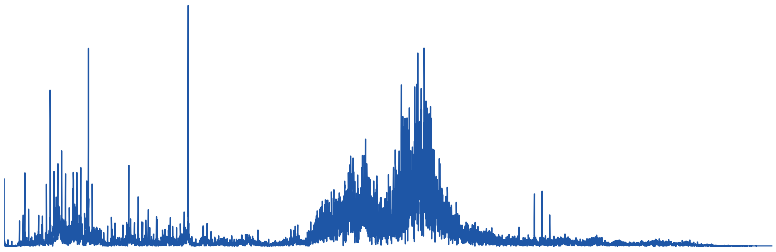

Figure 5. The FFT spectrum image of a ball fault signal.

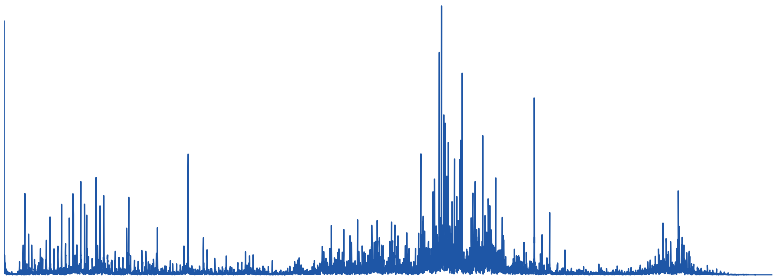

Figure 6. The FFT spectrum image of an outer-race fault signal

Table 2. The classification rate based on PCA with fault size being 0.014.

# of test	n[a]	Testing data				
		Test1(%)	Test2(%)	Test3(%)	Test4(%)	T(s)[b]
1	1	Load0(97.15)	Load1(99.95)	Load2(97.74)	Load3(93.41)	66
	3	Load0(98.15)	Load1(99.96)	Load2(99.99)	Load3(99.65)	80
	5	Load0(99.99)	Load1(100.00)	Load2(100.00)	Load3(100.00)	95
	10	Load0(100.00)	Load1(100.00)	Load2(100.00)	Load3(100.00)	145
2	1	Load0(83.80)	Load1(97.15)	Load2(100.00)	Load3(75.00)	64
	3	Load0(84.60)	Load1(100.00)	Load2(100.00)	Load3(75.04)	77
	5	Load0(86.40)	Load1(100.00)	Load2(100.00)	Load3(75.00)	92
	10	Load0(86.04)	Load1(100.00)	Load2(100.00)	Load3(75.00)	138
3	1	Load0(84.92)	Load1(99.76)	Load2(97.15)	Load3(76.05)	68
	3	Load0(86.17)	Load1(100.00)	Load2(100.00)	Load3(77.03)	80
	5	Load0(88.70)	Load1(99.96)	Load2(100.00)	Load3(75.26)	94
	10	Load0(89.45)	Load1(100.00)	Load2(100.00)	Load3(75.75)	144
4	1	Load0(96.56)	Load1(85.75)	Load2(98.30)	Load3(97.15)	66
	3	Load0(96.61)	Load1(86.81)	Load2(96.26)	Load3(100.00)	81
	5	Load0(97.70)	Load1(84.76)	Load2(97.30)	Load3(100.00)	97
	10	Load0(96.99)	Load1(77.72)	Load2(97.01)	Load3(100.00)	148

[a] n is the number of training samples per class, and the same below.
[b] T is the total time consumption of the processing program from *Eigen images Extraction* to *Fault Classification* for 20 times randomized tests, and the same below as well.

Table 3. The classification rate based on PCA with fault size being 0.021.

# of test	n[a]	Testing data				
		Test1(%)	Test2(%)	Test3(%)	Test4(%)	T(s)[b]
5	1	Load0(97.65)	Load1(99.13)	Load2(92.94)	Load3(87.22)	65
	3	Load0(97.92)	Load1(100.00)	Load2(98.83)	Load3(99.26)	80
	5	Load0(99.75)	Load1(98.67)	Load2(96.89)	Load3(97.28)	90
	10	Load0(99.75)	Load1(98.26)	Load2(97.35)	Load3(97.71)	134
6	1	Load0(99.66)	Load1(99.75)	Load2(90.36)	Load3(93.86)	66
	3	Load0(99.75)	Load1(100.00)	Load2(92.28)	Load3(97.06)	78
	5	Load0(99.75)	Load1(100.00)	Load2(93.99)	Load3(97.69)	92
	10	Load0(99.75)	Load1(100.00)	Load2(94.74)	Load3(96.66)	138
7	1	Load0(99.20)	Load1(98.33)	Load2(97.92)	Load3(99.76)	64
	3	Load0(99.61)	Load1(100.00)	Load2(100.00)	Load3(100.00)	77
	5	Load0(99.66)	Load1(100.00)	Load2(100.00)	Load3(100.00)	90
	10	Load0(99.75)	Load1(100.00)	Load2(100.00)	Load3(100.00)	132
8	1	Load0(99.72)	Load1(100.00)	Load2(99.41)	Load3(99.75)	65
	3	Load0(99.55)	Load1(100.00)	Load2(100.00)	Load3(100.00)	76
	5	Load0(99.65)	Load1(100.00)	Load2(100.00)	Load3(100.00)	91
	10	Load0(99.69)	Load1(100.00)	Load2(100.00)	Load3(100.00)	132

sampling number of each training class is equal to or greater than 5, most of the test cases could achieve a considerable classification rate in excess of 90%. Unfortunately two cases (marked with $\star$) are still around 75%, and the reason for this is similar to that discussed earlier.

It is worth mentioning that the time consumption of 2DPCA is considerably smaller than PCA, especially when n is larger. A detailed comparison is given in table 6. It is clear that 2DPCA method is more efficient than PCA method when using FFT spectrum images for fault diagnosis of bearings.

3.3. Discussion

The spectrum image of a given vibration signal is constructed based on FFT. In fact the spectrum is just a vector of amplitudes. Nevertheless it is not easy to mine useful knowledge

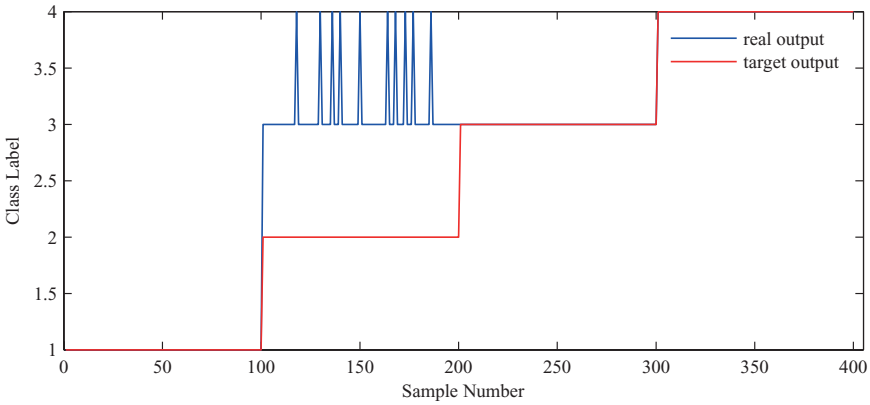

Figure 7. Actual output of Load1 for training and Load3 for testing with fault size being 0.014.

Table 4. The classification rate based on 2DPCA with fault size being 0.014.

		Testing data				
# of test	n[a]	Test1(%)	Test2(%)	Test3(%)	Test4(%)	T(s)[b]
1	1	Load0(99.97)	Load1(99.85)	Load2(99.41)	Load3(94.50)	51
	3	Load0(100.00)	Load1(100.00)	Load2(100.00)	Load3(99.95)	56
	5	Load0(100.00)	Load1(100.00)	Load2(100.00)	Load3(100.00)	63
	10	Load0(100.00)	Load1(100.00)	Load2(100.00)	Load3(100.00)	81
2	1	Load0(85.78)	Load1(100.00)	Load2(100.00)	Load3(75.45)*	50
	3	Load0(88.67)	Load1(100.00)	Load2(100.00)	Load3(75.00)*	56
	5	Load0(91.17)	Load1(100.00)	Load2(100.00)	Load3(76.46)*	63
	10	Load0(92.56)	Load1(100.00)	Load2(100.00)	Load3(78.26)*	81
3	1	Load0(87.79)	Load1(100.00)	Load2(100.00)	Load3(77.69)*	51
	3	Load0(91.56)	Load1(99.96)	Load2(100.00)	Load3(80.74)*	58
	5	Load0(92.24)	Load1(100.00)	Load2(100.00)	Load3(80.66)*	65
	10	Load0(93.45)	Load1(100.00)	Load2(100.00)	Load3(83.13)*	84
4	1	Load0(99.25)	Load1(86.17)	Load2(99.51)	Load3(100.00)	52
	3	Load0(99.55)	Load1(85.94)	Load2(99.47)	Load3(100.00)	59
	5	Load0(99.65)	Load1(84.63)	Load2(99.26)	Load3(100.00)	66
	10	Load0(99.89)	Load1(83.64)	Load2(99.53)	Load3(100.00)	85

directly from the vector. The spectrum image is a different view of the vector and provides a new way to extract information. We also carry out similar tests by taking FFT spectrum amplitudes as the features, where PCA and the same minimum distance method are used for fault classification. Similarly, after testing the performance of different dimension reduction with PCA and selecting the best case, the contribution of selected components with 90% is also designated in this section.

The results are shown in tables 7 and 8. Obviously the classification performance using FFT amplitude as features is inferior to that using the spectrum images, especially when the testing load condition is different from the training load condition.

Some other remarks are as follows.

(1) By comparing tables 2 and 3 with tables 4 and 5, it can be found that bearing fault diagnosis based on 2DPCA can achieve better performance than PCA in most cases.

(2) Time consumption of processing based on 2DPCA is much less than PCA, especially when the number of training samples per class is large.

(3) In general, a larger n could obtain a higher classification rate (see tables 2–5)). When using the spectrum image as the feature, an acceptable classification rate can still be achieved with only one single training image.

In order to illustrate the potential application of the proposed method in bearing fault diagnosis, a comparative study between the present work and published literature is presented in table 9. Adopting the same faulty bearing data collected from the Case Western Reserve University [25], most of the previous works considered only single load condition, where the training load condition and the testing load condition are the same. Only a few works evaluated the vibration data of multiple loading conditions. As shown in table 9, bearing fault diagnosis based on SLLEP under load 3hp condition, was

Table 5. The classification rate based on 2DPCA with fault size being 0.021.

# of test	n[a]	Testing data				
		Test1(%)	Test2(%)	Test3(%)	Test4(%)	T(s)[b]
5	1	Load0(99.75)	Load1(99.89)	Load2(96.91)	Load3(92.94)	52
	3	Load0(99.75)	Load1(100.00)	Load2(99.86)	Load3(100.00)	58
	5	Load0(100.00)	Load1(100.00)	Load2(100.00)	Load3(99.04)	65
	10	Load0(100.00)	Load1(100.00)	Load2(100.00)	Load3(100.00)	84
6	1	Load0(99.74)	Load1(100.00)	Load2(91.71)	Load3(95.45)	51
	3	Load0(99.75)	Load1(100.00)	Load2(96.70)	Load3(98.24)	58
	5	Load0(99.75)	Load1(100.00)	Load2(96.08)	Load3(99.95)	65
	10	Load0(99.75)	Load1(100.00)	Load2(99.25)	Load3(100.00)	84
7	1	Load0(99.75)	Load1(98.06)	Load2(100.00)	Load3(99.72)	50
	3	Load0(99.75)	Load1(100.00)	Load2(100.00)	Load3(100.00)	57
	5	Load0(99.75)	Load1(100.00)	Load2(100.00)	Load3(100.00)	63
	10	Load0(99.75)	Load1(100.00)	Load2(100.00)	Load3(100.00)	82
8	1	Load0(99.75)	Load1(100.00)	Load2(98.83)	Load3(100.00)	51
	3	Load0(99.75)	Load1(100.00)	Load2(100.00)	Load3(100.00)	58
	5	Load0(99.75)	Load1(100.00)	Load2(100.00)	Load3(100.00)	65
	10	Load0(99.75)	Load1(100.00)	Load2(100.00)	Load3(100.00)	83

Table 6. The time consumption diversity of Load0 as training with fault size being 0.014.

Training data	Testing data	n	T_{pca}(s)	T_{2dpca}(s)	$\triangle T$(s)[a]
Load0	Load0	1	68	51	17
		3	82	58	24
		5	96	64	32
		10	144	82	62
	Load1	1	71	52	19
		3	85	59	26
		5	95	65	30
		10	145	83	62
	Load2	1	65	51	14
		3	80	57	23
		5	99	64	35
		10	143	82	61
	Load3	1	66	51	15
		3	80	56	24
		5	95	63	32
		10	145	81	64

[a] $\triangle T = T_{\text{pca}} - T_{\text{2dpca}}$, that is: the time consumption difference between PCA and 2DPCA.

carried out to classify bearings with fault size being 0.021in using minimum-distance classifier in [27]. In [28], with FDF as feature, SVMs and fractal dimension were employed to diagnose the bearings with fault size being 0.014in and 0.021in. In [29], feature extraction based on LMD analysis method and MSE was put forward to perform fault diagnosis of bearings under load 3hp condition. In [30], bearings under load 2hp condition, were subjected to fault diagnosis based on multiscale permutation entropy (MPE) and improved support vector machine based binary tree (ISVM-BT). Moreover taking all load conditions into account, the improved distance evaluation technique and ANFIS were also employed to diagnose bearings with seven healthy cases in [31].

However the classification rate of the proposed method can achieve 100% in cases where the training and testing load condition are the same, as shown in tables 4 and 5. And the classification rate is still high when the training and testing load condition are different.

Table 7. The classification rate with FFT amplitude with fault size being 0.014.

# of test	n[a]	Testing data				T(s)[b]
		Test1(%)	Test2(%)	Test3(%)	Test4(%)	
1	1	Load0(85.51)	Load1(62.81)	Load2(67.84)	Load3(66.20)	10
	3	Load0(93.41)	Load1(63.69)	Load2(59.66)	Load3(61.17)	10
	5	Load0(96.78)	Load1(57.50)	Load2(54.91)	Load3(51.51)	10
	10	Load0(99.39)	Load1(51.25)	Load2(53.75)	Load3(50.00)	11
2	1	Load0(73.64)	Load1(99.09)	Load2(73.81)	Load3(73.04)	9
	3	Load0(76.31)	Load1(99.89)	Load2(75.00)	Load3(75.06)	9
	5	Load0(75.00)	Load1(100.00)	Load2(75.00)	Load3(75.00)	9
	10	Load0(75.00)	Load1(100.00)	Load2(75.00)	Load3(75.00)	11
3	1	Load0(77.81)	Load1(74.99)	Load2(90.99)	Load3(76.25)	9
	3	Load0(78.59)	Load1(74.17)	Load2(98.47)	Load3(77.01)	9
	5	Load0(76.65)	Load1(75.00)	Load2(99.91)	Load3(75.00)	10
	10	Load0(75.66)	Load1(75.00)	Load2(100.00)	Load3(75.00)	12
4	1	Load0(73.56)	Load1(75.00)	Load2(73.40)	Load3(97.61)	9
	3	Load0(74.86)	Load1(75.00)	Load2(75.00)	Load3(98.94)	9
	5	Load0(75.00)	Load1(75.00)	Load2(75.00)	Load3(99.01)	10
	10	Load0(75.00)	Load1(75.00)	Load2(75.00)	Load3(99.31)	11

Table 8. The classification rate with FFT amplitude with fault size being 0.021.

# of test	n[a]	Testing data				T(s)[b]
		Test1(%)	Test2(%)	Test3(%)	Test4(%)	
5	1	Load0(85.08)	Load1(58.45)	Load2(59.14)	Load3(60.05)	9
	3	Load0(95.58)	Load1(65.08)	Load2(68.80)	Load3(63.63)	9
	5	Load0(98.96)	Load1(66.78)	Load2(69.65)	Load3(65.17)	9
	10	Load0(99.76)	Load1(70.14)	Load2(72.04)	Load3(65.30)	10
6	1	Load0(66.04)	Load1(86.88)	Load2(70.35)	Load3(60.31)	8
	3	Load0(72.36)	Load1(97.33)	Load2(72.59)	Load3(67.45)	9
	5	Load0(74.40)	Load1(99.70)	Load2(72.86)	Load3(69.40)	9
	10	Load0(74.81)	Load1(99.99)	Load2(73.53)	Load3(70.94)	10
7	1	Load0(71.17)	Load1(69.04)	Load2(94.28)	Load3(64.80)	8
	3	Load0(74.74)	Load1(73.97)	Load2(99.99)	Load3(69.79)	9
	5	Load0(74.97)	Load1(74.95)	Load2(99.99)	Load3(71.80)	9
	10	Load0(75.08)	Load1(75.00)	Load2(100.00)	Load3(74.17)	10
8	1	Load0(73.40)	Load1(68.90)	Load2(71.17)	Load3(96.39)	9
	3	Load0(75.22)	Load1(75.15)	Load2(73.70)	Load3(96.99)	9
	5	Load0(75.50)	Load1(75.05)	Load2(75.42)	Load3(97.33)	9
	10	Load0(76.33)	Load1(75.00)	Load2(75.89)	Load3(99.70)	10

Table 9. Comparisons between the current work and some published work.

References	Load conditions	No. of training samples	Classification rate
Li *et al* [27]	Single	100	98.33%
Yang *et al* [28]	Single	118	95.253 % (0.014in) 99.368 % (0.021in)
Liu *et al* [29]	Single	15	100%
Li *et al* [30]	Single	80	100%
Lei *et al* [31]	Multiple	20	91.42%
The proposed method	Multiple	10	95.65% (0.014in) 99.90%(0.021in)

4. Conclusion

In this paper, spectrum images were proposed as the features for fault diagnosis of bearings. The spectrum images of vibration signals could be simply obtained through FFT. After processing with 2DPCA, the corresponding eigen images were extracted. The classification of faults was realized with a simple minimum distance criterion based on the eigen images. The effectiveness of the proposed method was demonstrated with experimental vibration signals. As a different view of FFT spectrum, the images could significantly improve the performance of fault diagnosis. When the training sample is very limited - e.g. only one training image - the proposed method can still achieve high accuracy.

Acknowledgments

The work was supported by National Natural Science Foundation of China (51475455), Natural Science Foundation of Jiangsu (BK20141127), the Fundamental Research Funds for the Central Universities (2014Y05), and the project funded by the Priority Academic Program Development of Jiangsu Higher Education Institutions (PAPD).

References

[1] Loparo K *et al* 2000 Fault detection and diagnosis of rotating machinery *IEEE Trans. Industrial Electron.* **47** 1005–14
[2] Liu X, Bo L, He X and Veidt M 2012 Application of correlation matching for automatic bearing fault diagnosis *J. Sound Vib.* **331** 5838–52
[3] Jalan A K and Mohanty A R 2009 Model based fault diagnosis of a rotor-bearing system for misalignment and unbalance under steady-state condition *J. Sound Vib.* **327** 604–22
[4] Bianchini C, Immovilli F, Cocconcelli M, Rubini R and Bellini A 2011 Fault detection of linear bearings in brushless ac linear motors by vibration analysis *IEEE Trans. Ind. Electron.* **58** 1684–94
[5] Link H, LaCava W, Van Dam J, McNiff B, Sheng S, Wallen R, McDade M, Lambert S, Butterfield S and Oyague F 2011 Gearbox reliability collaborative project report: findings from phase 1 and phase 2 testing *Contract* **303** 275–3000
[6] Randall R B and Antoni J 2011 Rolling element bearing diagnostics—a tutorial *Mech. Syst. Signal Process.* **25** 485–520
[7] Jardine A K S, Lin D and Banjevic D 2006 A review on machinery diagnostics and prognostics implementing condition-based maintenance *Mech. Syst. Signal Process.* **20** 1483–510
[8] Heng R B W and Nor M J M 1998 Statistical analysis of sound and vibration signals for monitoring rolling element bearing condition *Appl. Acoust.* **53** 211–26
[9] Samuel P D and Pines D J 2005 A review of vibration-based techniques for helicopter transmission diagnostics *J. Sound Vib.* **282** 475–508
[10] Khelf I, Laouar L, Bouchelaghem A M, Rémond D and Saad S 2013 Adaptive fault diagnosis in rotating machines using indicators selection *Mech. Syst. Signal Process.* **40** 452–68
[11] Chen X, Zhou J, Xiao J, Zhang X, Xiao H, Zhu W and Fu W 2014 Fault diagnosis based on dependent feature vector and probability neural network for rolling element bearings *Appl. Math. Comput.* **247** 835–47
[12] Wu J-D and Kuo J-M 2009 An automotive generator fault diagnosis system using discrete wavelet transform and artificial neural network *Expert Syst. Appl.* **36** 9776–83
[13] Li N, Zhou R, Hu Q and Liu X 2012 Mechanical fault diagnosis based on redundant second generation wavelet packet transform, neighborhood rough set and support vector machine *Mech. Syst. Signal Process.* **28** 608–21
[14] Xian G-M and Zeng B-Q 2009 An intelligent fault diagnosis method based on wavelet packer analysis and hybrid support vector machines *Expert Syst. Appl.* **36** 12131–6
[15] Li W, Zhu Z, Jiang F, Zhou G and Chen G 2015 Fault diagnosis of rotating machinery with a novel statistical feature extraction and evaluation method *Mech. Syst. Signal Process.* **50–1** 414–26
[16] Lei Y, Lin J, He Z and Zi Y 2011 Application of an improved kurtogram method for fault diagnosis of rolling element bearings *Mech. Syst. Signal Process.* **25** 1738–49
[17] Hong Z-Q 1991 Algebraic feature extraction of image for recognition *Pattern Recognit.* **24** 211–9
[18] Lee S-J, Jung S-B, Kwon J-W and Hong S-H 1999 Face detection and recognition using PCA in *TENCON 99. Proc. of the IEEE Region 10 Conf.* volume 1 pp 84–7
[19] Sun Q-S, Zeng S-G, Liu Y, Heng P-A and Xia D-S 2005 A new method of feature fusion and its application in image recognition *Pattern Recognit.* **38** 2437–48
[20] Toole A J, Phillips P J, Jiang F, Ayyad J, Penard N and Abdi H 2007 Face recognition algorithms surpass humans matching faces over changes in illumination *IEEE Trans. Pattern Anal. Mach. Intell.* **29** 1642–6
[21] Klein R, Masad E, Rudyk E and Winkler I 2014 Bearing diagnostics using image processing methods *Mech. Syst. Signal Process.* **45** 105–13
[22] Griffaton J, Picheral J and Tenenhaus A 2014 Enhanced visual analysis of aircraft engines based on spectrograms *ISMA2014* pp 2809–22
[23] Yang J, Zhang D, Frangi A F and Yang J-Y 2004 Two-dimensional PCA: a new approach to appearance-based face representation and recognition *IEEE Trans. Pattern Anal. Mach. Intell.* **26** 131–7
[24] Wang L, Zhang Y and Feng J 2005 On the Euclidean distance of images *IEEE Trans. Pattern Anal. Mach. Intell.* **27** 1334–9
[25] Case Western Reserve University Bearings vibration dataset available: http://csegroups.case.edu/bearingdatacenter/home (accessed October 2015)
[26] Abdi H and Williams L J 2010 Principal component analysis *Wiley Interdiscip. Rev.: Comput. Stat.* **2** 433–59
[27] Li B and Zhang Y 2011 Supervised locally linear embedding projection (SLLEP) for machinery fault diagnosis *Mech. Syst. Signal Process.* **25** 3125–34
[28] Yang J, Zhang Y and Zhu Y 2007 Intelligent fault diagnosis of rolling element bearing based on SVMs and fractal dimension *Mech. Syst. Signal Process.* **21** 2012–24
[29] Liu H and Han M 2014 A fault diagnosis method based on local mean decomposition and multi-scale entropy for roller bearings *Mech. Mach. Theory* **75** 67–78
[30] Li Y, Xu M, Wei Y and Huang W 2016 A new rolling bearing fault diagnosis method based on multiscale permutation entropy and improved support vector machine based binary tree *Measurement* **77** 80–94
[31] Lei Y, He Z and Zi Y 2008 A new approach to intelligent fault diagnosis of rotating machinery *Expert Syst. Appl.* **35** 1593–600